

MICROFABRICATION WITH FEMTOSECOND LASER PROCESSING

Michelle Griffith, Pin Yang, George Burns, and Marc Harris

Sandia National Laboratories
Albuquerque, NM 87815

Abstract

Our research investigates the special characteristics of femtosecond laser processing for microfabrication. The ultrashort pulse significantly reduces the thermal diffusion length. As a result, material is removed more efficiently with little damage to the surrounding feature volume. Currently, we are exploring the basic mechanisms that control femtosecond laser processing, to determine the process parameter space for laser processing of metals to address manufacturing requirements for feature definition, precision and reproducibility. One of the unique aspects to femtosecond radiation is the creation of localized structural changes. By scanning the focal point within a transparent material, we can create three-dimensional waveguides.

This paper will describe our results to explore femtosecond laser ablation for laser processing of metals and glasses. We will discuss the effect of laser parameters on removal rate, feature size/definition, aspect ratio, material structure, and performance. Examples of component fabrication in metals and glasses will be shown.

Introduction

At Sandia National Laboratories, miniaturization dominates future hardware designs, and technologies that address the manufacture of micro-scale to nano-scale features are in demand. Currently, Sandia is developing technologies such as photolithography/etching (e.g. silicon MEMS)¹, LIGA², micro-electro-discharge machining (micro-EDM)³, and focused ion beam (FIB) machining⁴ to fulfill some of the component design requirements. As in the macro world, no one micro- or nano-scale process can do it all. Some processes are more encompassing than others, but each process has its niche, where all performance characteristics cannot be met by one technology. For example, micro-EDM creates highly accurate micro-scale features but the choice of materials is limited to conductive materials. With silicon-based MEMS technology, highly accurate nano-scale integrated devices are fabricated but the mechanical performance may not meet the requirements. Femtosecond laser processing has the potential to fulfill a broad range of design demands, both in terms of feature resolution and material choices, thereby improving fabrication of micro-components. One of the unique features of a femtosecond laser is the ability to ablate nearly all materials with little heat transfer⁵, and therefore melting or damage, to the surrounding material, resulting in highly accurate micro-scale features.

For many years, Sandia has been involved in the development of laser-based rapid prototyping (RP)⁶ and direct fabrication technologies⁷⁻⁹ to build prototype parts, as well as small lot production components. The significant aspect of these technologies is the utilization of a computer model, sliced into two-dimensional cross-sections, to drive the fabrication process,

where a part is fabricated layer by layer to create the three-dimensional shape. For example, we use these models to routinely fabricate polymeric three-dimensional representations for design verification and, in some instances, fabricate patterns for investment casting to obtain a metal component. Instead of using secondary processes, such as investment casting, to fabricate the final metal part, Sandia has developed a laser-based metal fabrication technology, known as Laser Engineered Net Shaping (LENS[®])⁷, to directly fabricate the metallic component. These technologies have greatly enhanced our ability to quickly fabricate parts but the size regime is typically on the macro-scale. The RP polymeric-based technologies are now scaled to the micro level but their properties do not typically meet the performance requirements of components that are of interest to Sandia. The LENS[®] process can produce parts down to the mm-scale but no smaller due to processing constraints.

At present, Sandia is developing a femtosecond laser micro-fabrication capability to expand into the micro-scale size regime for metals and glasses. We hope to produce accurate, reliable micro-components. To facilitate adoption of this technology in the manufacturing environment, further understanding is required to ensure routine fabrication of robust components with desired material properties. This requires understanding and control of the material behavior during part fabrication. This paper describes our initial research to understand the ablation process of stainless steel to determine the correct path sequencing to drive the process in order to fabricate components with clean surfaces and accurate features. The paper will also describe our work to understand the modification of glass structures and control of this phenomenon to fabricate waveguides and other photonic device based features.

Experimental Setup

Figure 1 is a photo of our femtosecond laser micro-fabrication system. We are using a Hurricane femtosecond laser from Spectra-Physics. This laser provides a small footprint which is more amenable for the manufacturing environment with the following characteristics: 800 nm wavelength, 120 fs pulse width, 1 KHz frequency, up to 1 mJ energy, and approximately 4 mm output beam. This beam is transferred to the working envelope by a series of mirrors and is focused with a microscope objective. The beam is focused onto the working surface and X-Y stages manipulate the geometry in the plane, whereas the microscope objective is mounted to a Z stage to manipulate the beam position.

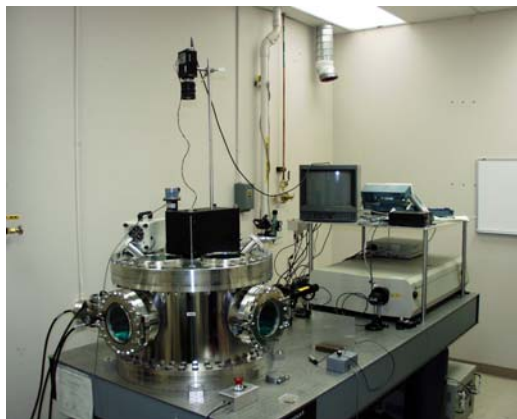


Figure 1. Sandia's femtosecond laser micro-fabrication system.

Stainless steel 304L foils were used for the metal work. Typically, 50-200 micron thick foils were used. The foils were mounted into a picture frame holder, where features ablated through thickness easily fall out of the foil for analysis. A 20X objective was used resulting in a minimum spot size of 60 microns at 975 mW. Smaller spot sizes are easily obtainable, but for this work a larger spot size was used to aid in understanding the ablation process. Full power (975 mW) was used for most studies. Since this work involves the utilization of traditional RP techniques, effects of travel velocity, layer decrement, and geometric features were studied. Sandia-developed software was used to define the path sequence for part fabrication. Simple machine language (M and G codes) was used for initial parameter studies. Ablated features were analyzed by optical and scanning electron microscopy. Width and depth of features were measured by interferometry techniques.

When our femtosecond laser was used to modify the local glass structure, the power of laser beam had to be reduced to prevent optical damages to the glass. The energy of the beam was first reduced by rotating a half wave plate together with a thin film polarizer along the beam path. Further energy reduction was accomplished by the use of neutral density filters. The glass used in this evaluation was a thermally treated chemical vapor deposited (CVD) amorphous quartz (Quartz International, Albuquerque, NM). The laser beam was directed through a long-working-distance microscope objective (Mitutoyo, NIR 20X, NA = 0.40) and focused into the polished glass approximately 500 to 750 μm below the surface. Typical laser energy per pulse used in this investigation was controlled between 0.45 to 0.9 μJ . The samples were scanned perpendicular to the focused fs laser pluses at a rate of 20 $\mu\text{m/s}$ to create micron-sized lines inside the bulk glass. The optical properties of these scanned lines were studied using near-field and far-field techniques. Light scattering in these modified regions (waveguides) was determined by image analysis of light intensity decay along the beam direction, using a digital camera. Laser-induced birefringence was characterized by using a Dalsa CA-D1-0128T camera attached to an Olympus transmitted light microscope (BH-2) with samples between crossed polars on a rotation stage. Digital signals from these images were processed using a National Instruments PCI-1424 digital image capture card and software written in LabVIEW G code.

Results in Metals

A. Ablation Properties

For complex part fabrication, we will need to process parts in a layered manufacturing approach. Much of our understanding of ablation with respect to velocity and layer decrement for stainless steel can be found in the following reference¹⁰. By utilizing a layered manufacturing approach, a three-dimensional shape is represented by two-dimensional cross-sections where each cross-section is represented by a raster pattern. There are two choices for volumetric material removal: 1) fast travel velocity and smaller layer decrement or 2) slow travel velocity and larger layer decrement. Processing speed is of great importance in the manufacturing environment, but so is final part resolution and cleanliness. For this work, all studies were done in air, where it is generally more difficult for the species to ablate away from the surface resulting in redeposition onto the sidewalls or top surfaces. It is beneficial to process

in air for a variety of factors from simpler equipment (no vacuum/gas handling equipment) to easy sample exchange. Other researchers have found techniques¹¹ to provide good feature definition without species redeposition while processing in air. Appropriate techniques will be incorporated into our system in the future.

In order to correctly choose the layer thickness and raster width (known as hatch) we need to understand the effect of velocity on feature width and depth. Initially, single lines, 10 mm long, were drawn at various velocities and their width and depth measured using interferometry. A foil thickness of 50 microns was used for this study. Figures 2a and 2b show the measured ablated depth and channel width. As expected, the depth decreases as the velocity increases from 46 microns to 5 microns for a change in velocity from 0.4 mm/s to 3.4 mm/s. At slower velocities, one would expect the channel width to match closely to the minimum spot size, 60 microns, and decrease in width as the velocity increases. In Figure 2b, the data shows this general trend within error. Inconsistencies are most likely due to species redeposition thereby adding measurement error depending on the efficiency or inefficiency of removal.

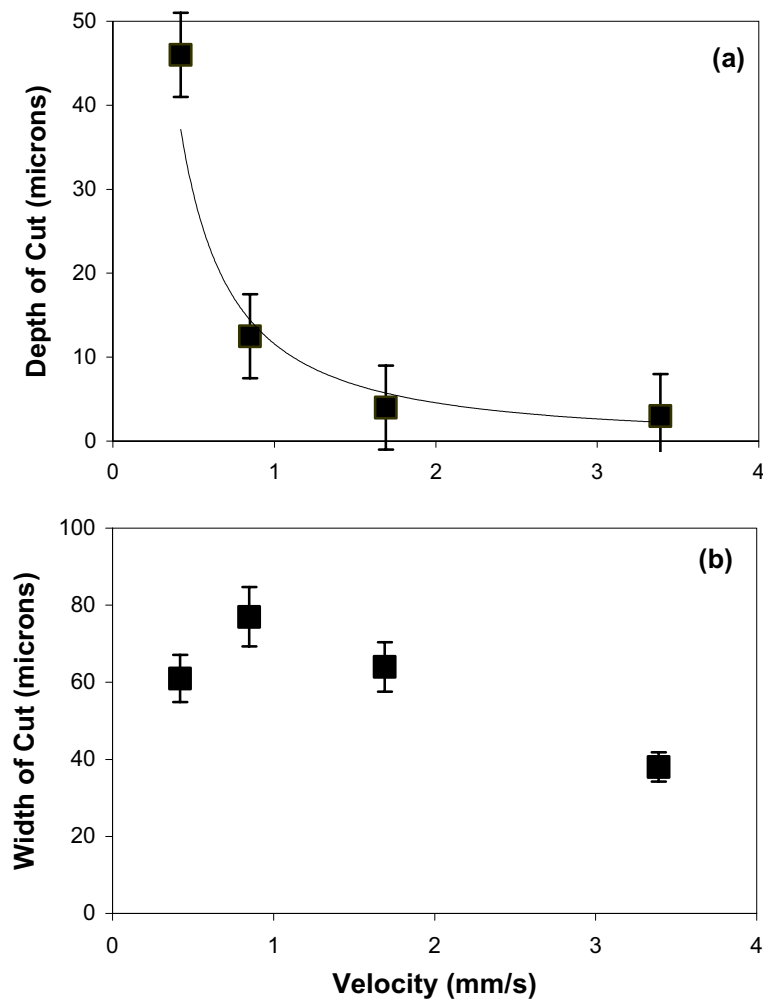


Figure 2. Ablated depth (a) and channel width (b) for lines processed at four travel velocities at 975 mW. A 50 μ m foil thickness was used in this study.

B. Components

With the knowledge of depth and width at various velocities, complex shapes were tried. For manufacturing speed, it would be best to utilize the greatest decrement possible, or try to match the 46 micron cut shown in the previous section. Since Figure 2A shows a dramatic change in depth for a small change in velocity at low travel speeds, a decrement value of 25 microns was chosen at a speed of 0.4 mm/s. Figure 3 shows the results for a comb-like geometry that was cut into a 200 micron thick SS304 foil. Comb arms are 200 microns wide with 250 micron spacing. The comb geometry is reasonably accurate dimensionally, but as the figure shows, there is a large amount of recast material along the sidewalls. Furthermore, it took twelve passes to ablate through the thickness or a discrepancy of 100 microns. This discrepancy can be explained by the ablation energy being utilized to remove old material that has recast within the channel.

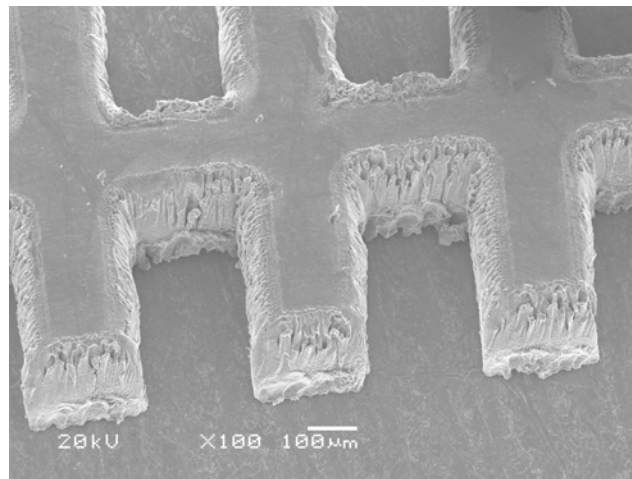


Figure 3. Comb geometry fabricated at 0.42 mm/s with 25 micron layer decrements.

In contrast, Figure 4 shows clean and accurate features for a ratchet gear fabricated with 5 micron decrements using a travel velocity of 1.7 mm/s. The gear was cut through a 100 micron thick foil in 18 passes, or 90 microns, resulting in a more efficient process where energy is directly utilized to cut features. Even though the gear was cut from a 100 micron foil, it is apparent that the small layer increment is better for part fabrication. For this parameter set, the particles can volatilize away from the channel without heavy plasma shielding or increased particle-particle collisions.

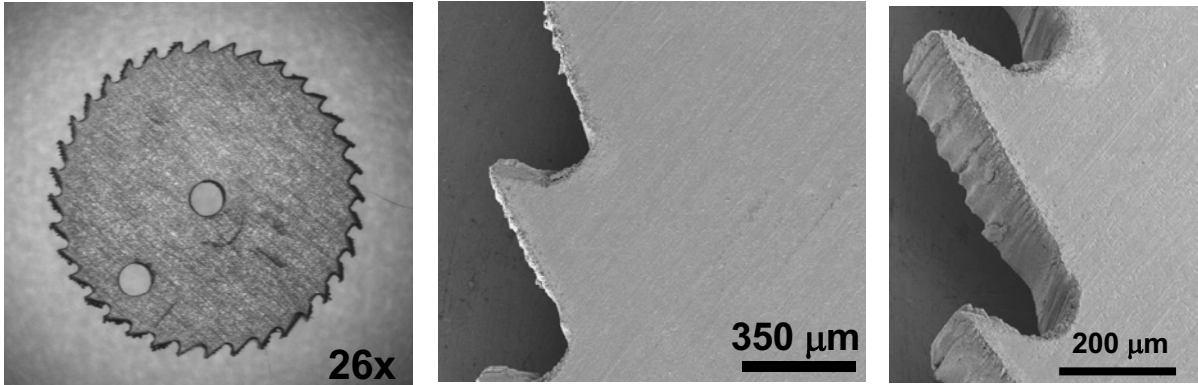


Figure 4. Ratchet gear fabricated in 100 micron thick SS304 foil using the following parameters: 1.69 mm/s travel velocity and 5 micron layer decrement.

Results in Glasses

A. Structure Modification

When an intense femtosecond laser pulse is focused inside bulk glass, the intensity in the local volume can become high enough to cause absorption through nonlinear processes, leading to optical breakdown or photo-damage. Slightly below the optical breakdown threshold, this nonlinear, multi-photon absorption can locally alter the glass structure and cause refractive index changes.¹²⁻¹⁶ If the intensity of the laser is below the threshold level of multi-photon absorption, glass becomes almost transparent to the laser beam. Therefore, it is important to identify the proper processing space that can effectively increase the refractive index without creating photo-damage in the bulk glass. Figure 5 shows the micro-Raman spectrum of bulk silica glass and normalized spectrum of a laser-damaged region (0.1 mJ). Under cross-polarized light condition, the damaged regions exhibit stress birefringence and are occasionally associated with microcracks. Without the normalization procedure, the intensity of the Raman bands from the laser-damaged region is consistently less than that from the bulk glass. This reduction in intensity indicates that the modified regions have structures of lower density where some glass has been partially replaced by voids. However, this reduction in intensity becomes significantly less for laser-modified regions (0.9 μ J) that produce refractive index change without creating stress birefringence. Furthermore, the normalized Raman spectra show an increase in the 490 and 605 cm^{-1} peaks in the damaged region, indicating an increase in the number of 4- and 3-membered ring structures in the silica network. The formation of these 4- and 3- ring structures are sometimes associated with the creation of new quasi-surfaces at small voids in the silica-rich matrices.¹⁸ In addition, the Raman band peaking between 400 and 500 cm^{-1} is significantly narrower in the spectra from laser modified regions compared to the bulk glass. The relative narrowness of the bands in the spectra indicates that the silica networks in these areas have a smaller distribution of ring sizes, with fewer large rings. This type of modification of the silica network is typically achieved by quick melting followed by fast re-solidification during the laser process.

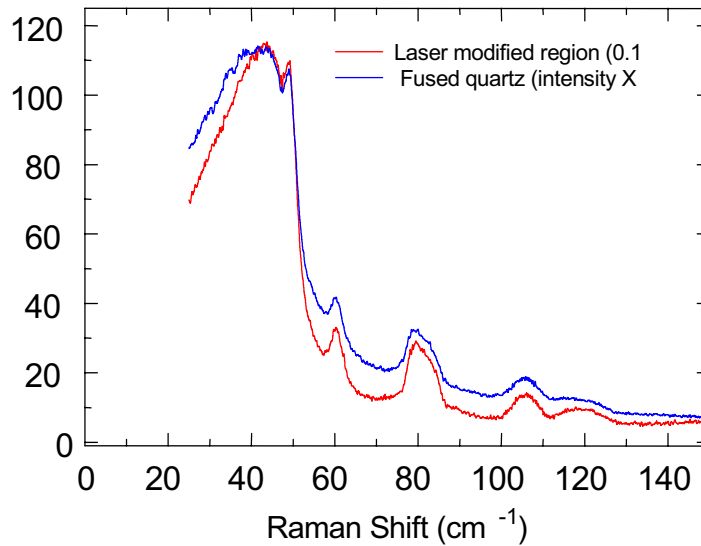


Figure 5. Micro-Raman spectra for bulk glass and laser modified regions.

B. Components

With the knowledge of the effect of average laser power on structure modification of glass, direct writing waveguides inside amorphous quartz was explored. Figure 6 shows the top view, near-field and far-field patterns of laser-modified lines above (0.1 mJ) and below photo-damage threshold (0.9 μ J). The near-field and far-field patterns were obtained from the transmitted beams at 650 nm through 2 mm length of laser-modified regions. The near-field pattern of waveguides created below damage threshold illustrates the propagation of a single LP₀₁ mode through the waveguide inside of a bulk glass. The far-field pattern indicates that this transmitted mode possesses a nearly Gaussian profile. Above the photo-damage threshold (> 2.2 μ J), extensive light scattering is observed, which is consistent with the Raman analysis results where some glass has been partially replaced by voids. Experimental results suggest that these laser-modified regions have a unique biaxial optical birefringence, where the maximum birefringence is in the range of 0.002 to 0.004. Figure 7 (a) illustrates the variation in transmitted light intensity through the laser-modified regions under cross-polarized light. The polarization direction of the laser beam was systematically rotated 10° from spot to spot. The observation of an optical extinction for every 90° suggests that the laser-modified regions possess an optical birefringence property. Furthermore, the sinusoidal variation of the transmitted light intensity (see Fig. 7 (b)) is consistent with the theoretical prediction of a birefringent material. Results indicate that the laser-induced birefringence property in the bulk glass can be controlled by laser power level, accumulated exposure, and polarization direction of the writing laser.¹⁹ Details of the creation of birefringence by the femtosecond laser pulse will be reported elsewhere.¹⁹

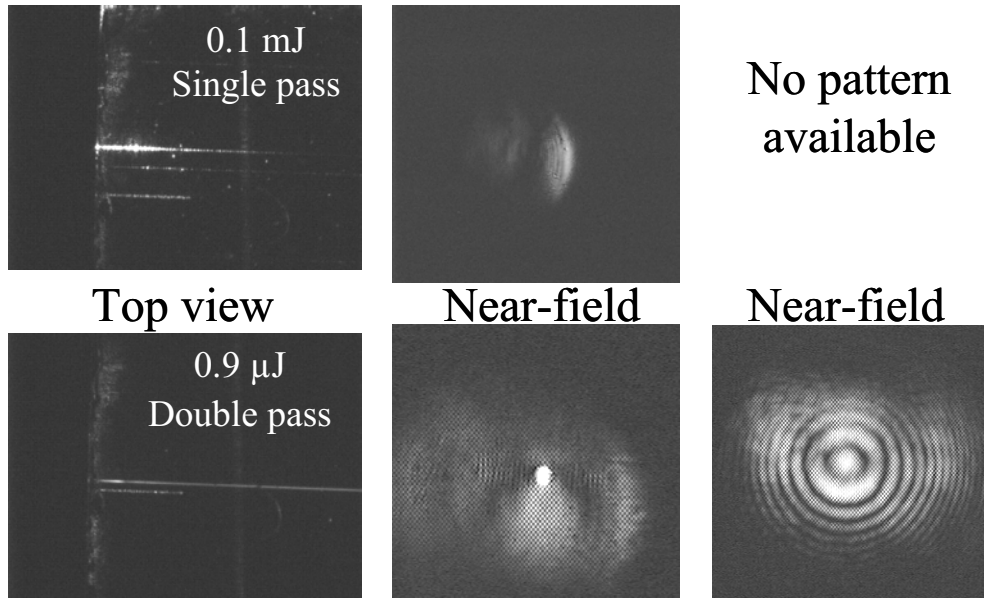


Figure 6. Direct-write buried waveguides in glass by femtosecond pulse laser. The top and bottom images are regions modified above and below the photo-damage threshold, respectively.

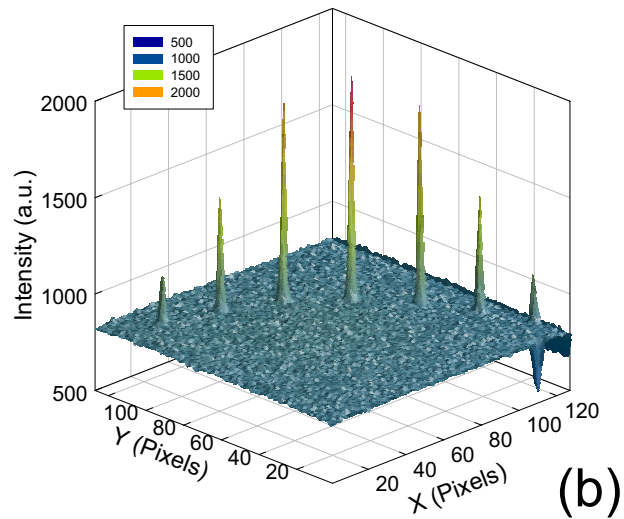
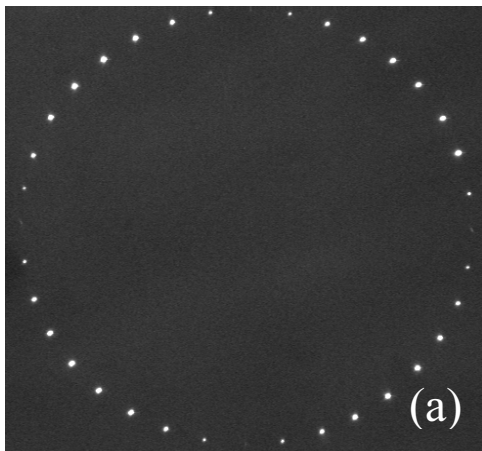


Fig. 7 (a) Transmission image of laser modified regions under a cross polarized light, the polarization direction of the laser beam is rotated 10° for each modification, (b) the change of transmitted light intensity in the first quarter.

Conclusions

Initial studies show that femtosecond laser processing is a promising manufacturing technology to fabricate micro-components. We have demonstrated with a basic understanding of travel velocity and layer decrement on resulting channel morphology, complex shapes can be fabricated in stainless steel. A key factor in producing clean features is choosing the correct layer decrement that allows the ionized species to escape the channel. Using a unique non-linear absorption behavior, we have demonstrated that femtosecond laser pulses, when properly adjusted, can locally modify the glass structure and directly fabricate waveguides in bulk glass. Results show these laser-modified regions possess an optical birefringence property which can be controlled by the polarization direction of the laser beam. The capability of creating and controlling birefringence properties in glass by laser processing could have significant implications for the development of novel optical devices.

Acknowledgments

This work supported by the U. S. Department of Energy under contract DE-AC04-94AL85000. Sandia is a multiprogram laboratory operated by Sandia Corporation, a Lockheed Martin Company, for the United States Department of Energy.

References

1. J. J. Sniegowski, "Moving the World with Surface Micromachining," *Solid State Technology*, February Issue, pp. 83-90. 1996.
2. J. Hruby, "LIGA Technology and Applications", *MRS Bulletin*, Vol. 26, No. 4, p. 337, 2001.
3. G. L. Benavides, L. F. Bieg, M. P. Saavedra, E. A. Bryce, "High Aspect Ratio Meso-scale Parts Enabled by Wire Micro-EDM", *Journal of Microsystems Technologies*, Vol. 8, No.6, p. 395, 2002.
4. D.P. Adams, G.L. Benavides, "Micrometer-scale Machining of Metals and Polymers Enabled by Focused Ion Beam Sputtering", *Materials Research Society, V546, Symposium O Proceedings, April 1999*, pp. 201-205, 1999.
5. B. N. Chichikov, C. Momma, S. Nolte, F. von Alvensleben, A. Tunnermann, "Femtosecond, Picosecond, and Nanosecond Laser Ablation of Solids", *Appl. Phys. A* 63, pp. 109-115, 1996.
6. C. L. Atwood, M. C. Maguire, M. D. Baldwin, "RP&M Applications at Sandia National Laboratories", *Stereolithography and Other RP&M Technologies*, Society of Manufacturing Engineers, Dearborn, Michigan, pp. 253-272, 1996.
7. M. L. Griffith, M. T. Ensz, J. D. Puskar, C. V. Robino, J. A. Brooks, J. A. Philliber, J. E. Smugeresky, W. H. Hofmeister, "Understanding the Microstructure and Properties of Components Fabricated by Laser Engineered Net Shaping (LENS)", *Materials Research Society, V625, Symposium Y Proceedings, April 2000*, pp. 9-20. 2000.

8. M. L. Griffith, M. T. Ensz, D. L. Greene, D. E. Reckaway, J. A. Romero, T. B. Crenshaw, L. D. Harwell, T. E. Buchheit, and V. Tikare, "Solid Freeform Fabrication using the WireFeed Process", *Proceedings of the Solid Freeform Fabrication Symposium, August, 1999*, University of Texas, Austin, TX, pp.529-536, 1999.
9. J. Cesarano, R. Seglaman III, P. D. Calvert, "Robocasting Provides Moldless Fabrication from Slurry Deposition", *Ceramic Industry 148*, pp. 94-102, 1998.
10. M. L. Griffith, M. T. Ensz, D. E. Reckaway, *Femtosecond Laser Machining of Steel*, Proceedings of SPIE Photonics West 2003: Laser Applications in Microelectronics and Optoelectronic Manufacturing VIII, to be published by SPIE, Bellingham, WA, 2003.
11. S. Nolte, C. Momma, G. Kamlage, A. Ostendorf, C. Fallnich, F. von Alvensleben, H. Welling, "Polarization Effects in Ultrashort-pulse Laser Drilling", *App. Phys. A 68*, pp.563-567, 1999.
12. K. Miura, J. Oiu, H. Inouye, and T. Mitsuyu, "Photowritten Optical Waveguides in Various Glasses with Ultrashort Pulse Laser", *Appl. Phys. Lett. 71*, pp.3329-3331, 1997.
13. D. Homoelle, S. Wielandy, A. L. Gaeta, N. F. Borelli, and C. Smith, "Infrared Photosensitivity in Silica Glasses Exposed to Femtosecond Laser Pulses", *Opt. Lett. 24*, pp. 1311-1313, 1999.
14. S. Cho, H. Kumagai, K. Midorikawa, and M. Obara, "Time-Resolved Dynamics of Plasma Self-Channeling and Bulk Modification in Silica Glasses Induced by a High-Intensity Femtosecond Laser", *First International Symposium on Laser Precision Microfabrication, V4088, Proceedings of SPIE, June 2000*, pp. 40-43, 2000.
15. C. B. Schaffer, J. F. Garcia, and E. Mazur, "Bulk Heating of Transparent Materials Using a High-Repetition-Rate Femtosecond Laser", *Appl. Phys. A 76*, pp.351-354, 2003.
16. J. W. Chan, T. R. Huser, S. H. Risbud, and D. M. Krol, "Modification of the Fused Silica Glass Network Associated with Waveguide Fabrication Using Femtosecond Laser Pulses", *Appl. Phys. A 76*, pp.367-371, 2003.
17. K. Miura, J. Qiu, T. Mitsuyu, and K. Hirao, "Preparation and Optical Properties of Fluoride Glass Waveguides Induced by Laser Pulses", *J. Non-Cryst. Solids 256&257*, pp. 212-219, 1999.
18. D. R. Tallant, B. C. Bunker, C. J. Brinker, and C. A. Balfe, "Raman Spectra of Rings in Silicate Materials", *Materials Research Society, V73, Symposium Y Proceedings, November 1986*, pp. 261-267. 1986.
19. P. Yang, G. R. Burns, J. Guo, T. S. Luk, and A. G. Vawter, "Femtosecond Laser Pulse Induced Birefringence in Optically Isotropic Glass", submitted to *Appl. Phys. Lett.*, 2003.